misorientation in other directions. Especially when the beam is finely collimated such a misorientation will affect the domain distribution $N(\varepsilon_1)$ and its neglect is therefore not justifiable.

It is satisfying that, in cases where a distinction can be made, partial R values favor the T.N. model, in agreement also with experimental measurements of the pronounced variation of the diffracted intensity of a boracite on rotation around the diffraction vector (Thornley & Nelmes, 1974).

Finally, it may be pointed out that though the physical formulation of extinction requires further study, the present theory extends the domain of applicability of an extinction refinement. This is of special importance in neutron diffraction studies, where extinction is often severe. In further development of formalisms it may be necessary to modify or abandon the mosaic model, and to allow for the partial coherence of the multiple diffraction process.

The authors would like to thank Drs F. K. Larsen and W. R. Busing for making the neutron data on $LiTbF_4$ and $LiOH.H_2O$ available prior to publication and Mrs L. Marshall for assistance with the calculations. They are indebted to a referee for many helpful comments. Support of this work by the National Science Foundation is gratefully acknowledged.

References

ALCOCK, N. W. (1971). *Acta Cryst.* B**27**, 1682–1683.
ALS-NIELSEN, J., HOLMES, L. M., LARSEN, F. K. & GUGGENHEIM, H. J. (1975). *Phys. Rev.* B. In the press.
BECKER, P. J. (1973). These d'Etat. Paris.
BECKER, P. J. & COPPENS, P. (1973), 1st European Crystallography Conference, Bordeaux, France.
BECKER, P. J. & COPPENS, P. (1974*a*). *Acta Cryst.* A**30**, 129–147.
BECKER, P. J. & COPPENS, P. (1974*b*). *Acta Cryst.* A**30**, 148–153.
BECKER, P. J., COPPENS, P. & ROSS, F. K. (1973). *J. Amer. Chem. Soc.* **95**, 7604–7609.
COPPENS, P. (1974). *Acta Cryst.* B**30**, 255–261.
COPPENS, P. & HAMILTON, W. C. (1970). *Acta Cryst.* A**26**, 71–83.
DELAPLANE, R. G. & IBERS, J. A. (1969). *Acta Cryst.* A**25**, 2423–2437.
HAMILTON, W. C. (1957). *Acta Cryst.* **10**, 629–634.
NELMES, R. J. (1969). *Acta Cryst.* A**25**, 523–526.
THORNLEY, F. R. & NELMES, R. J. (1974). *Acta Cryst.* A**30**, 748–757.
WEBER, K. (1963). *Acta Cryst.* **16**, 535–542.
ZACHARIASEN, W. H. (1967). *Acta Cryst.* **23**, 558–564.

Acta Cryst. (1975). A**31**, 425

Structure of X-ray Wave Packets in Perfect and Highly Distorted Crystals

BY F. BALIBAR & C. MALGRANGE

Laboratoire de Minéralogie-Cristallographie associé au C.N.R.S., Université Paris VI, *Tour* 16, 4 *place Jussieu*, 75230 *Paris Cedex* 05, *France*

(*Received* 6 *January* 1975; *accepted* 31 *January* 1975)

It is shown that, in order to treat the problem of the propagation of an X-ray wave in a distorted crystal, the plane-wave assumption, which is one of the fundamental ingredients in the usual dynamical theory, should be removed. Both the incident and the crystal waves should be built as *wave packets*, *i.e.* continuous distributions of **K** vectors, characterized by their extensions in both reciprocal and direct spaces. The characteristic structure of the crystal wave packet for a perfect crystal, and the changes undergone by this structure as a result of the crystal distortions, are examined; the criterion for the validity of geometrical optics is thus reformulated.

I. Introduction

The dynamical theory of X-ray diffraction is generally considered to be concerned with the problem of propagation of an electromagnetic wave of given frequency falling in the X-ray region in a medium made up of a more-or-less perfect three-dimensional array of atoms. As a matter of fact, the papers which originated this kind of studies (Ewald, 1916; Darwin, 1914; von Laue, 1931) were only concerned with a very special kind of waves (*i.e.* plane waves) incident on a perfect crystal (*i.e.* a medium without any disturbance in the three-dimensional ordering of atoms). The wave inside the crystal then appears as a superposition of *four plane waves*, the characteristics of which can be fully determined from the boundary conditions at the entrance surface. It was soon realized that in order to deal with real cases one has to extend this ideal treatment (which we shall call the Ewald–Laue theory) to that of a non-plane wave travelling in a non-perfect crystal. This has usually been performed by mere adaptation of the ideal plane-wave solution: the characteristic parameters of the plane-wave solution (*e.g.* the departure from exact Bragg angle) were considered to be space varying and one calculated the change of this 'variable constant' necessary to match the real propagation conditions. Kato's (1963, 1964*a*, *b*), Penning's (1961) and Penning & Polder's (1966) treatments can be considered as typical examples of such a way of dealing with the real problem. For ten

years or so, it has come to be realized that this treatment is not able to take into account all observable effects; in particular, the phenomenon of creation of new wave fields cannot be satisfactorily handled along these lines. In this respect Takagi's (1962, 1969) theory and Taupin's (1964) theory appear to be more useful. In these 'general' theories, the wave inside the crystal is no longer viewed as a plane wave, changing from place to place but still locally plane, as in the previous extensions of the Ewald–Laue theory, but as an amplitude-modulated wave. It is then possible to take into account effects such as diffraction by highly distorted regions and the related phenomenon of creation of new wave fields (Balibar & Authier, 1967; Balibar, 1968, 1969; Authier & Balibar, 1970).

We feel that the time has come to look at the problem from the opposite direction; *i.e.* we feel that a proper treatment of propagation of an electromagnetic wave in a crystal – be it perfect or not – should proceed from the more general to the more particular case, rather than in the reverse and historical order; in other words, we should consider the Ewald–Laue treatment as a special case of a general solution, rather than exhibit the general solution by tackling the Ewald–Laue solution in order to increase its range of validity. Takagi's treatment of the crystal wave as a modulated wave represents one step in this direction; we want to go further and reformulate the dynamical theory from the start. In this respect we must represent the crystal wave as a more general type of wave, *i.e.* as a wave packet (note that a modulated wave is a special case of a wave packet).

We shall therefore be concerned here with the study of the shape of the crystal wave packet induced by a vacuum wave packet in a crystal of a general type. In the first part we shall show that, owing to the three-dimensional periodic structure (it must not be forgotten that the main characteristic of the medium is its periodicity, even if this periodicity is somehow broken; a crystal, even imperfect, is always, to a first-order approximation, characterized by a three-dimensional periodic structure), the crystal wave packet exhibits some general features. The problem (studied in the second part) is then to determine how the characteristics of the gross structure of the wave packet will be affected by irregularities in the periodicity of the medium, in other words by crystal distortions. We shall show that by mere comparison of some length characteristic of both the wave packet extension and the crystal distortion itself, it is possible to predict all the known phenomena occuring in real crystals, including the so-called 'creation of new wave fields'.

II. Wave packets – modulation due to extension in real- and reciprocal-space

It is well known that in considering the propagation of X-radiations in crystals it is not necessary to keep track of the vectorial character of the fields; it is sufficient to consider the scalar quantities obtained by projection of the fields on the plane of incidence and perpendicular to it. Under such conditions, any part of the considered wave can be represented by a square integrable function of space and time: $\psi(x,y,z,t)$. A further simplification ensues from the fact that the radiation frequency is kept constant; therefore we need not take into consideration any time dependence –

$$\psi(x,y,z,t) \rightarrow \psi(x,y,z).$$

Now, application of the Fourier integral theorem ensures that any vector belonging to the vector space of square integrable functions can be written as a continuous linear combination of eigenfunctions of the type $\exp(i\mathbf{k} \cdot \mathbf{r})$. Since this is the mathematical form corresponding to the usual concept of a *plane* wave, any scalar wave can be viewed as a *superposition of plane waves*, of different $\mathbf{k}$ vectors (wave vectors). Such a superposition is usually called a *wave packet*.

Two important concepts in the consideration of wave packets are those of *extension in real space* and *extension in reciprocal space*. The wave packet extension in reciprocal space is the range in the directions of reciprocal space covered by the $\mathbf{k}$ vectors entering the plane-wave expansion of the considered wave packet. It is well known that, for a given direction of reciprocal space, this quantity Δk_{x_i} is related to the spatial extension Δx_i of the wave packet in the corresponding

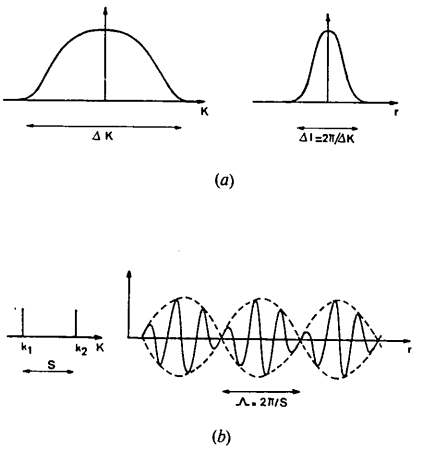

Fig. 1. Localized phenomenon *versus* modulated phenomenon. (*a*) A space-localized phenomenon along one space direction (call it r) corresponds to a continuous distribution of wave-vectors along the corresponding k direction in reciprocal space. This distribution extends over a finite range Δk (left part of the figure). The corresponding amplitude distribution is that of a localized phenomenon for which a characteristic width $\Delta l = 2\pi/\Delta k$ can be defined (right part of the figure). (*b*) Space-modulated phenomenon corresponds to the superposition of two individual plane waves; the corresponding k distribution is made up of two δ functions centred on points $k=k_1$ and $k=k_2$ ($S=|k_1-k_2|$). The corresponding amplitude distribution exhibits a modulation for which a characteristic modulation wavelength may be defined: $\Lambda = 1/|k_2-k_1| = 1/S$. Note that this amplitude distribution extends over infinity.

three dimensions of real space, through

$$\Delta k_{x_i} \cdot \Delta x_i \simeq 2\pi\,, \quad x_i = x, y \text{ or } z\,. \tag{1}$$

Note that this relation is a direct consequence of the fact that the expansion of the wave packet in plane waves is obtained by Fourier transformation of $\psi(x,y,z)$.

One must be somewhat careful in interpreting the physical meaning of the concept of extension in real space. In priniciple, this concept refers to the fact that the considered phenomenon does not extend over all space but is localized in a definite region of volume ($\Delta x \Delta y \Delta z$), because plane waves of slightly different wave vectors give rise to destructive interference except in a very localized region [Fig. 1(*a*)]. In the X-ray case, we have to deal with a steady flow of photons (or radiation); it means that there exists a mean direction of propagation (call it z); the proper concept is then that of wave front. Relations (1) state that the wave front perpendicular to the mean direction of propagation z is not infinite but of limited *width* $\Delta x \Delta y$ (an infinite width would correspond to $\Delta k_x = \Delta k_y = 0$ and therefore, since $\Delta k_z \simeq 0$, to a single plane wave and to the usual picture of an infinite plane wave. In other words, in any xy plane the intensity is zero outside a 'beam' of width $\Delta x \Delta y$.

The physical situation is somewhat different when the wave-vector distribution in a given direction $\mathbf{k}$ of reciprocal space does not correspond to a continuous distribution extending over a certain Δk but to only two components $\mathbf{k}_1$ and $\mathbf{k}_2$ separated by a distance $S = |\mathbf{k}_2 - \mathbf{k}_1|$; [Fig. 1(*b*)]. It is then impossible to find regions along the corresponding direction of the real space (call it r) where destructive interference occurs; the phenomenon has an infinite extension in r, but its amplitude is *modulated*. Interference between the two components $\mathbf{k}_1$ and $\mathbf{k}_2$ results in *beats*; the wave is then characterized by:

– a fast oscillation of spatial frequency equal to the mean frequency of the two components, $(k_1 + k_2)/2$

– a larger oscillation, or modulation, superimposed on the first one, the frequency of which is half the difference between the component frequencies: $|k_1 - k_2|/2 = S/2$. The resultant phenomenon appears as a sinusoidal wave with modulated amplitude: the rate of the modulation (or modulation wavelength) in the direction r is defined as $\Lambda = 2\pi/S$ [Fig. 1(*b*)].

In summary, combination of a *continuous* spectrum (of extension Δk) of plane waves gives rise to a *localized phenomenon* of finite width $2\pi/\Delta k$ [Fig. 1(*a*)], while combination of two separate waves a distance S apart in reciprocal space gives rise to a *modulated phenomenon* of modulation wavelength $2\pi/S$ [Fig. 1(*b*)].

In fact there is no clear-cut limit between the second case (two plane waves with two different $\mathbf{K}$ separated by a distance S, resulting in an infinite modulated phenomenon) and the first case (a continuous distribution of $\mathbf{K}$ ranging over a certain ΔK). One goes gradu-

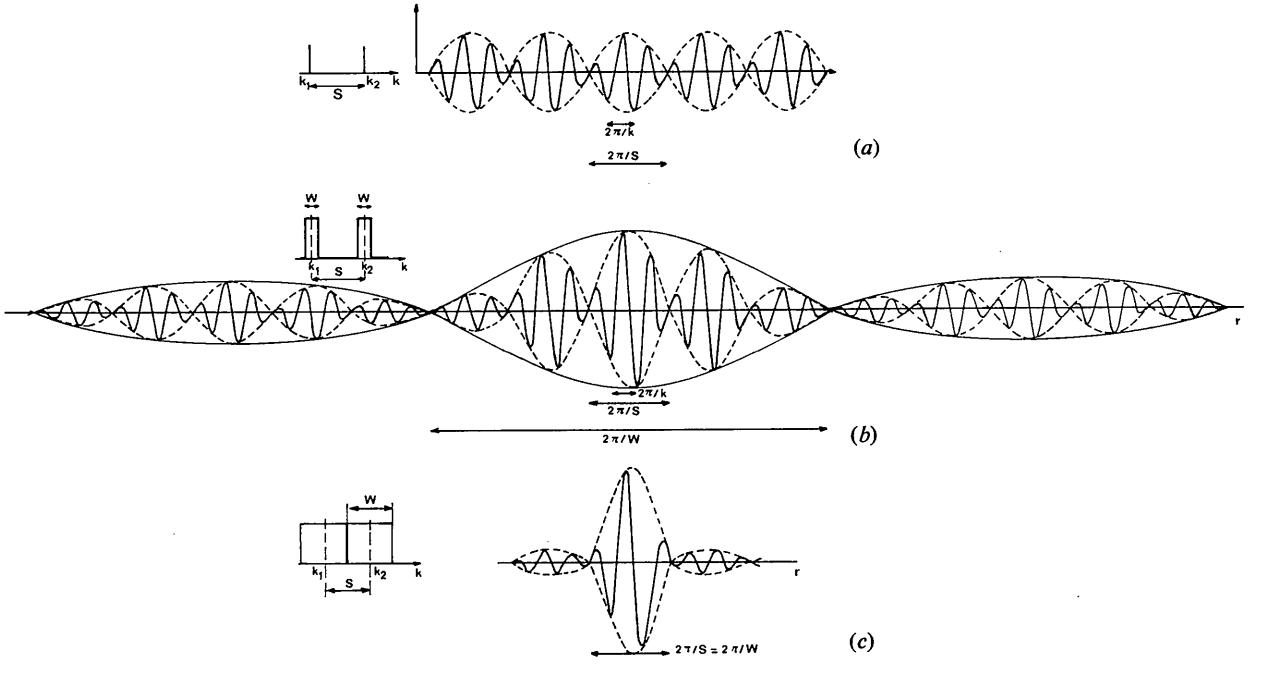

Fig. 2. Transition from modulation to localization. Intermediate situations between those pictured in Fig. 1(*a*) and Fig. 1(*b*) can be obtained by letting the two wave-vector distributions of Fig. 1(*b*) get larger and larger, until they rejoin and become one single distribution. The corresponding amplitude distributions exhibit a gradual change from a modulated phenomenon extending to infinity to a more and more localized phenomenon. For $S = W$, the modulation wavelength becomes equal to the extension $2\pi/W$ of the wave-packet; modulation disappears.

ally from one type of effect to the other by letting the two distribution functions corresponding to the second case get larger and larger and form what we might call 'subwave packets' (Fig. 2). A modulation effect is bound to occur as long as the finite size of each subwave packet (as determined by the *width W* of each K distribution) is larger than the modulation length (determined by the *separation S* between the two sub-distributions). In other words, in order to know the physical structure of a wave packet made of two separated subwave packets, it is necessary to consider the ratio $\varrho = W/S = (\textit{width of each subwave packet})/(\textit{separation between these subwave packets})$ (in reciprocal space).

We shall see below that this situation is precisely the one encountered in the case of X-ray propagation in crystals.

III. Structure of the crystal wave packet induced in a perfect crystal by an incident vacuum wave

Let $\psi_0^{(i)}(r)$ be a vacuum incident wave of the most general type. Thanks to the Fourier integral theorem this wave may be described as a superposition of plane waves. The only plane waves which are bound to propagate with a noticeable amplitude in the crystal are those with wave vectors lying within a very small angle around the Bragg direction θ_B (here $\Delta\theta$ is the width of the rocking curve). Therefore, the structure in reciprocal space of the incident vacuum packet is the one of a wave packet centred around a mean direction (let us call it $\overrightarrow{OP_0^{(i)}}$) of the wave vectors. The vacuum wave-vector distribution is thus characterized by (see Fig. 3):

- a zero spread in the direction $OP_0^{(i)}$
- a non-zero spread $\delta K_0^{(i)}$ in the direction T_0 perpendicular to $\overrightarrow{OP_0^{(i)}}$; $\delta K_0^{(i)}$ varies between 0 and $\simeq K\Delta\theta$, where $K = 2\pi/\lambda_0$ (λ_0: vacuum wavelength).

The corresponding amplitude distribution is:

$$\psi_0^{(i)}(\mathbf{r}) = \int_{\delta K_0(i)} A_0^{(i)}(\mathbf{K}^{(i)}) \exp\left[i(\mathbf{K}^{(i)} \cdot \mathbf{r})\right] d\mathbf{K}^{(i)}, \quad (2)$$

where $\mathbf{K}^{(i)}$ represents a wave vector originating at 0 and with extremity lying on T_0 within $\delta K_0^{(i)}$.

From the Ewald–Laue treatment, we know how each of the plane components of this wave packet will be transformed on entering the crystal; each one will give rise to four plane waves, the wave vectors of which are fully determined by the usual technique, from the knowledge of the dispersion surface and of the direction normal to the entrance surface of the crystal.

The crystal wave packet is then obtained by combining all the crystal plane waves thus induced by each of the components, $\exp(i\mathbf{K}^{(i)} \cdot \mathbf{r})$, of the incident vacuum wave packet. We now want to determine the structure of this wave packet, *i.e.* its extension in both reciprocal and direct spaces.

Let us first recall that in both reciprocal and direct spaces, we need only consider two dimensions, those corresponding to the plane of incidence in real space. Let z be the direction in this plane along the reflecting planes and x the direction perpendicular to it (Fig. 4). Let K_z and K_x be the corresponding directions in reciprocal space. It must be emphasized that the usual picture of the dispersion surface does not represent the reciprocal space proper, since two different origins (O and G) have been chosen for the wave vectors; when looking at the extension of the crystal wave packet, especially in the K_x direction, one must 'develop' the usual picture in order to refer all wave vectors to the same origin. This procedure is exemplified in Fig. 4(*a*) and (*b*), in the case of the four plane waves induced by one single component of the incident vacuum packet. Fig. 5 shows the distribution in **K** vectors obtained when dealing with the more general case of an incident wave packet characterized by its spread $\delta K_0^{(i)}$ along T_0. The composition of the crystal wave packet is determined by the fact that the X-rays are elastically diffracted by the atoms of the crystal; in other words, that all the extremities of the wave vectors of its plane-wave components must lie on the dispersion surface, which is in fact a cut at $E =$ const. of a hypersurface $f(E, \mathbf{K}_0, \mathbf{K}_g)$ (see Stern, Pendry & Boudreaux, 1969). Fig. 5, developed as in Fig. 4, will show that for a vacuum wave packet of size

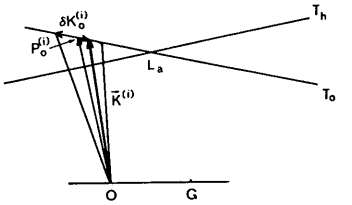

Fig. 3. Structure of the vacuum incident wavepacket. $OL_a = 2\pi/\lambda_0$; λ_0 = vacuum wavelength. $\delta\theta^{(i)} = (\overrightarrow{OP_0^{(i)}}, \overrightarrow{OL_a})$ = mean departure from the Bragg angle of the incident wave.

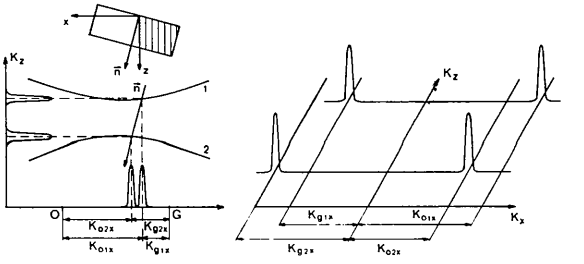

(*a*) (*b*)

Fig. 4. Representation in reciprocal space of the wave packet induced in a perfect crystal by a single plane wave. In the standard representation (*a*) (dispersion surface picture), the wave vectors may originate either at O or G). In the wave-packet representation (*b*), the wave-vector distribution of the considered wave must be referred to the same origin; it is then made out of four δ functions.

$\delta K_0^{(i)}$, the induced distribution of **K** vectors in reciprocal space is made of four 'bumps' two along each direction K_x and K_z.

III. 1 *Wave-packet structure along K_x and x*

(*A*) *Along the K_x direction*, the two bumps are separated by a distance which is approximately $|\overrightarrow{OG}| = 4\pi \sin\theta/\lambda$ (Fig. 4), where λ is the crystal wavelength. Since the dispersion surface is fairly parallel to the K_x axis, the width of each bump is approximately $\delta K_0^{(i)} \cos\theta_B$, being therefore independent of the departure from the Bragg angle θ_B. $\delta K_0^{(i)} \cos\theta_B$ in turn is always less than $K\Delta\theta = (2\pi/\lambda)\Delta\theta (\delta K_0^{(i)} \lesssim K\Delta\theta$ and $\cos\theta_B \leq 1$). Therefore a rough estimate of the ratio $\varrho = W/S$ yields $\varrho \lesssim \Delta\theta/\sin 2\theta \simeq 10^{-4}$, for the K_x distribution.

(*B*) The structure of the crystal wave packet *along the x direction* can be then inferred from the results of § II.

(*a*) Because of the small value of the ratio W/S the two subwave packets behave as plane waves, beating with each other. This results in a modulation which is just what is at the origin of the Borrmann effect in the case of an Ewald–Laue wave field. Nevertheless, owing to the structure of the original wave packet, each of these subwave packets has a structure determined both by the structure of the original vacuum wave packet and the relative weight allowed by the usual Ewald–Laue theory to the plane waves excited by each individual component.

(*b*) The spatial width of the beam is expected to be $2\pi/\delta K_0^{(i)} \cos\theta_B$, with a minimum value of $2\pi/K\Delta\theta \cos\theta_B$, corresponding to the case of a spherical wave in vacuum. In this case the spatial width of the beam is $\simeq$ (Pendellösung length) $\times$ tg θ_B.

(*c*) For each of these subwave packets, the position inside the Borrmann fan is obtained by looking for each z, at the position of the maximum of the amplitude distribution in real space (also called the centre of the subwave packet).

This position is calculated classically by using the stationary-phase method since the maximum of the amplitude corresponds to those points in real space where the interference is the most constructive, *i.e.* those points where the phase is stationary.

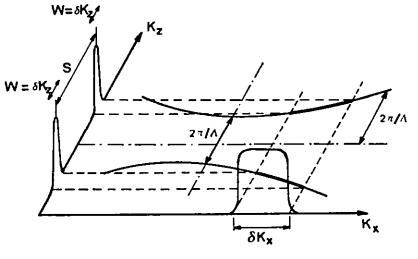

Fig. 5. Wave-vector distribution along axes K_z and K_x corresponding to an incident vacuum wave packet of finite extension. This picture, once developed as in Fig. 4, would give rise to two 'bumps' along each direction K_z and K_x.

III. 2 *Wave-packet structure along K_z and z*

(*A*) For a given width $\delta K_0^{(i)}$ of the incident vacuum wave packet, the separation *and* width of the corresponding two bumps of the distribution of wave vectors *along* K_z in the crystal are very much dependent on $\delta\theta^{(i)}$, the mean departure from the exact Bragg angle of the vacuum wave packet under consideration (Fig. 3).

The bump separation S varies continuously from $2\pi/\Lambda$, for $\delta\theta^{(i)} \simeq 0$ (Λ = Pendellösung wavelength), to $(2\pi/\Lambda) + K\Delta\theta \sin\theta_B$, for $\delta\theta^{(i)} = \Delta\theta$. Replacing $K\Delta\theta$ by its value $2\pi/\Lambda \sin\theta_B$ yields:

$$2\pi/\Lambda \leq \text{bump separation } S \leq 2 \times 2\pi/\Lambda \,. \qquad (3)$$

The width W of each bump also depends on $\delta\theta^{(i)}$. For a given $\delta K_0^{(i)}$, its minimum value is obtained for $\delta\theta^{(i)} = 0$. From the analytic equation of the hyperbolic dispersion surface in the (K_x, K_z) space, this minimum value is evaluated as

$$\frac{1}{2}\frac{2\pi}{\Lambda}\frac{\mathrm{tg}^2\theta_B}{(2\pi/\Lambda)^2}[\delta K_0^{(i)}]^2 \cos^2\theta_B = \tfrac{1}{2}\sin^2\theta_B \frac{1}{2\pi/\Lambda}[\delta K_0^{(i)}]^2 \,.$$

The maximum value of each bump width is obtained for $\delta\theta^{(i)} = \infty$ and is just $\delta K_0^{(i)} \sin\theta_B$. Therefore

$$\frac{1}{2\pi/\Lambda}[\delta K_0^{(i)}]^2 \sin^2\theta_B \lesssim \text{bump width } W \lesssim \delta K_0^{(i)} \sin\theta_B \,. \qquad (4)$$

Note that since $\delta K_0^{(i)}$ is always less than $K\Delta\theta$ ($= 2\pi/\Lambda \sin\theta_B$), $\delta K_0^{(i)} \sin\theta_B$ is always less than $2\pi/\Lambda$. Therefore the ratio ϱ is always less than one. It ranges from

$$\varrho = \left(\frac{\delta K_0^{(i)} \sin\theta_B}{2\pi/\Lambda}\right)^2 = \left(\frac{\delta K_0^{(i)}}{K\Delta\theta}\right)^2 \quad \text{for} \quad \delta\theta^{(i)} \simeq 0$$

to

$$\varrho = \tfrac{1}{2}\frac{\delta K_0^{(i)}}{K\Delta\theta} \quad \text{for} \quad \delta\theta^{(i)} \simeq \infty$$

$$\left(\frac{\delta K_0^{(i)}}{K\Delta\theta}\right)^2 \lesssim \varrho \lesssim \tfrac{1}{2}\frac{\delta K_0^{(i)}}{K\Delta\theta} \,. \qquad (5)$$

Fig. 6 shows the evolution of the K_z distribution; we show two cases $\delta\theta^{(i)} = 0$ and $\delta\theta^{(i)} = \Delta\theta$, for a given $\delta K_0^{(i)}$. We see that even for a very narrow $\delta K_0^{(i)}$ combination with an Ewald–Laue wave field (corresponding to two infinitely narrow bumps along K_z) is not always valid; this approximation is mainly justified for $\delta\theta^{(i)} \simeq 0$. As we go over to larger departures from the Bragg angle the K_z distribution loses its resemblance to an Ewald–Laue wavefield.

An extreme and important case is that of a spherical incident wave. Then $\delta K_0^{(i)} = K\Delta\theta$ and the width of each bump is equal to $2\pi/\Lambda$. Since the separation of

the bumps is at least $2\pi/\Lambda$ (Fig. 5) [*cf.* equation (3)] the situation is the one pictured in Fig. 6(*c*). Note that even in this case the ratio of width to separation is still less than one; the two bumps are neatly separated.

(*B*) From this last remark we conclude that *along the z direction*, the structure of the perfect crystal wave packet will always exhibit a *modulation* (which can be characterized by its *modulation length* Λ) superimposed on a fast oscillation of spatial periodicity λ.

Let us look more closely at what happens in the preceding extreme case (spherical incident wave). Each bump of the K_z distribution corresponds in real space to a subwave packet of size Λ [*cf.* equation (1)]. Since the modulation wavelength is also equal to Λ we are in a situation where the modulation effect is bound to disappear (*cf.* end of § II). Let us anticipate the next section; imagine that, for some reason or other, the separation between points I_1 and I_2 (Fig. 6) can become less than $2\pi/\Lambda$. Then the modulation effect would tend to disappear; as a matter of fact there would be beats and destructive interference between components belonging to two different subwave packets; this effect, which does not occur for $I_1I_2 \geq 2\pi/\Lambda$ because the separation is too large, results in a disturbance of the modulation, since modulation is the result of beats between components belonging to close different subwave packets.

However, that the distance I_1I_2 be equal to $2\pi/\Lambda$ (and not less), in other words the existence of a gap of finite width, is precisely what characterizes the perfect periodic crystal, as is well known from band theory; we may conclude that the *existence of a modulation of periodicity Λ is what characterizes the propagation of X-ray waves in a perfect crystal.* We can already predict that the main effect of crystal distortions will be to *perturb and even destroy* the modulation along the z direction. Note that, on the other hand, the modulation along x will not be sensitive to crystal deformations; the ratio W/S is less than 10^{-5} for a perfect crystal; it will eventually increase when there are some distortions because the separation OG between the two bumps in reciprocal space will change, but this change will never be important enough to modify sensibly the ratio W/S; in any case, W/S will never get to unity.

We may summarize the preceding discussion as follows: in a perfect crystal, the specific structure of the crystal wave is one of a modulated *Bloch wave packet*. Here 'Bloch wave' refers to the strong coupling between components with wave vectors differing by a reciprocal-lattice vector (resulting in a modulation of periodicity λ perpendicular to the reflecting planes). 'Modulated' refers to the modulation in the other direction (what is called the Pendellösung effect in the case of an incident single plane wave); these modulations imply that the crystal wave packet exhibits a structure in *separated sub*wave packets along each direction in reciprocal space.

From now on, we shall adopt the following terminology:

– Modulated Bloch wave packet = wave inside the crystal

– *Subwave packet* along x or z = amplitude (or intensity) distribution of X-rays corresponding to *one bump* in the K_x or K_z distribution. A modulated Bloch wave packet is the result of interference between these subwave packets.

IV. Structure of the crystal wave packet induced in a distorted crystal by an incident vacuum wave

IV. (*A*) *Effect of the distortions on the reference frame in reciprocal space*

As is usually done, we consider only those deformations for which it is possible to define a 'local reciprocal lattice'. Let $\mathbf{u}(\mathbf{r})$ be the displacement of an atom at $\mathbf{r}$, and $\mathbf{r}_0$ be the position vector of the point where the atom which is displaced to $\mathbf{r}$ by the distortion was originally located.

$$\mathbf{r} = \mathbf{r}_0 + \mathbf{u}(\mathbf{r}_0) \,. \tag{6}$$

Several authors (Kato, 1963; Penning & Polder, 1961) have shown that a local reciprocal-lattice vector $\mathbf{g}'$ can be defined in the vicinity of in the distorted crystal by

$$\mathbf{g}'(\mathbf{r}) = \mathbf{g} - \nabla[\mathbf{g} \,.\, \mathbf{u}(\mathbf{r}_0)] \,. \tag{7}$$

$\mathbf{g}'$ is now a function of position $\mathbf{r}$ inside the crystal. Therefore the reciprocal space is locally defined: for any point inside the crystal the K_z and K_x axes lie along and perpendicular to $\mathbf{g}'$ respectively. We now have to deal with a *varying reference frame in reciprocal space*. It is convenient, when describing the propagation of the crystal wave, to keep O fixed and let G change from place to place.

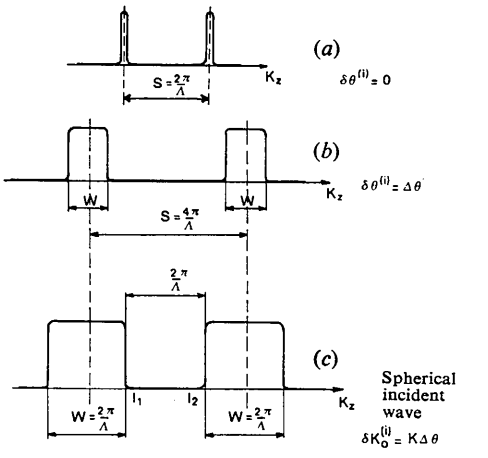

Fig. 6. Dependence of the K_z distribution on $\delta\theta_i$ (mean departure of the incident wave from exact Bragg angle). (*a*) and (*b*) For large departures, the width W of the K_z distribution may be fairly large, as compared to their separation S. (*c*) Extreme case of a spherical incident vacuum wave; W/S is still less than one.

Relation (7) is the starting point for the introduction of the concept of the ideal asymptotic crystal: for any position **r** inside the crystal one can imagine an ideal perfect crystal for which the reciprocal-lattice vector for the considered reflexion could be precisely **g'** (**r**); such an ideal crystal extends to infinity but still coincides in the vicinity of **r** with the real crystal; in this sense it is locally 'asymptotic' to the real crystal. For each of these perfect ideal crystals there exists in reciprocal space a 'local ideal dispersion surface'.

For a given **r** inside the crystal, this surface must be drawn in the local reciprocal space, *i.e.* in the local reference frame; it is then a hyperbola with axes along the local K_x and K_z. When going from one point **r** to another **r'** the geometrical characteristics of this hyperbola are maintained, since these do not depend on the strain (θ_B is roughly the same and the distance between the two apices is unchanged); but the axes of symmetry of the hyperbolae have changed, along with the reference frames. Nevertheless, since all hyperbolae have the asymptote parallel to the vacuum dispersion surface T_0 in common, the change of the crystal dispersion surface may be thought of (in our picture where O has been kept fixed) as a shift along T_0 (Fig. 7). The shift τ along T_0 between two positions of the hyperbola corresponding to a rotation of angle $\delta\theta$ of the reference frame in reciprocal space is given by:

$$\tau = K\delta\theta \,. \tag{8}$$

If we are now interested in the propagation of an X-ray wave between **r** and **r'** in a *continuously** distorted crystal, we must consider the whole continuous family of hyperbolae ranging from H to H' (Fig. 7). Let τ be the total shift along T_0; since τ is proportional to $|\mathbf{r}-\mathbf{r}'|$ and to the rate of deformation, the significant parameter is the value of the gradient of τ, *i.e.*

$$\frac{\partial\tau}{\partial|\mathbf{r}-\mathbf{r}'|} = \frac{\partial(K\delta\theta)}{\partial|\mathbf{r}-\mathbf{r}'|} \,. \tag{9}$$

Since

$$\delta\theta = \frac{1}{\sin 2\theta_B}\frac{1}{R}\frac{\partial}{\partial S_h}(\mathbf{h}\,.\,\mathbf{u}) \tag{10}$$

we see that the important parameter is the second derivative f of (**g** . **u**).

* By 'continuously' distorted crystal, we mean a crystal where $f=\partial\mathbf{g}\,.\,\mathbf{u}/\partial S_0\partial S_k=\text{const}$ (see Fig. 7). This is of course a very special case. But for our purpose (*i.e.* estimation of the strength of the deformations) it will be sufficient.

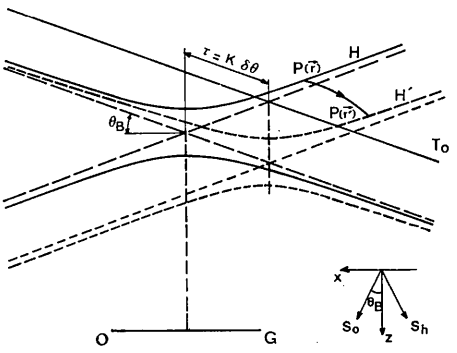

Fig. 7. When going from **r** to **r'**, the extremity P of a given wave vector OP moves across the whole family of hyporbolae which fills the gap between H and H'; the exact trajectory from $P(\mathbf{r})$ to $P(\mathbf{r}')$ depends on the precise form of the deformation.

IV (*B*) *Effect of distortions on a modulated-Bloch-wave packet*

Let us now consider a modulated-Bloch-wave packet, such as described in § III, travelling in a region of good crystal and arriving in a region containing distortions. The wave vectors of the various plane wave components are submitted to the change in reference frame described in § IV (*A*). If we adopt the point of view of a dispersion surface 'gliding' along T_0, we may consider that only one extremity P (Fig. 7) of each **K** vector moves while going through the distorted region. The trajectory of this extremity will depend on the geometrical characteristics of the crystal deformation. Several assumptions have been made concerning the way P moves (Penning & Polder, 1961; Penning, 1966; Kato, 1963*a*,*b*, 1964). For our purpose, we need not know precisely what this trajectory is, while going from **r** to **r'**; suffice it to know that the displacement of the local ideal characteristic point P will be of the same order of magnitude as τ, though it may not be exactly the same for all points P and may vary with the position of P on the local ideal dispersion surface. This displacement in P results in a shift $\tau\cos\theta_B$ along the K_x axis and a shift $\tau\sin\theta_B$ along the K_z axis; the shift is generally more noticeable along K_x than along K_z.

If we now consider the total K_x and K_z distributions corresponding to the considered modulated-Bloch-wave packet, we see that going from **r** to **r'** in the distorted crystal corresponds, for either K_x or K_z, to a global shift (either $\tau\cos\theta_B$ or $\tau\sin\theta_B$) of the two bumps of the K_x (or K_z) distribution.

We shall now show that the effect of this global shift on the structure of the modulated-Bloch-wave packet is threefold:

(*a*) a shift in *position* of the centre of each subwave packet;

(*b*) a *change* in the shape of each of these subwave packets; this change will affect the amplitude distribution both along x and z;

(*c*) but in the z direction it may be strong enough so as to eventually *destroy the modulation* along z which we have said to be characteristic of the propagation in real crystals.

(*a*) *Shift in position of the centre of each subwave packet*

A global shift $\tau\cos\theta_B$ in the K_x distribution (or a shift $\tau\sin\theta_B$ in the K_z distribution), implies a multipli-

cation by a phase factor $\exp(i\tau \cos\theta_B x)$ [or $\exp(i\tau \sin\theta_B z)$] of the corresponding distribution of amplitude.

Let us first consider the distribution of amplitude in the x direction. For a given z, we have identified the x position of the centre of each subwave packet with the energy trajectory (or 'beam' position) which is obtained through the stationary phase method. When we multiply the amplitude distribution along x by a factor $\simeq\exp(i\tau \cos\theta_B x)$, we add a quantity $\tau \cos\theta_B$ to the function which has to be stationary. This results in a change of the abscissa of the stationary point.

The same holds for the amplitude distribution along z; nevertheless the shift in position of the energy trajectory in this direction is less noticeable since the shift in the K_z distribution is tg θ_B times the one in the K_z distribution.

In brief, if it is still possible to define subwave packets (we shall see in a moment that the structure of the subwave packets may be destroyed) the trajectory of these subwave packets, or beams, will be modified by the crystal distortions. For a Bragg–Laue type of wave we usually say that the wave fields are curved.

(b) Change in shape of each subwave packet

Let us first consider the K_z distribution and the corresponding distribution of amplitude in the z direction. Moreover we shall assume that the crystal is made up of two parts; a perfect part where the K_z distribution is the one described in § III, and a distorted region. We shall concentrate on what happens to a single subwave packet travelling in the distorted region.

We must first acknowledge that, unlike in the perfect region, it is no longer possible to characterize *once and for all* the K_z distribution corresponding to the subwave packet under consideration (what we called a 'bump').

This is possible in the perfect crystal only because what happens along z over a distance Λ is repeated over and over identically; in other words, because we need not then consider the whole infinite crystal and may use a 'reduced scale' Λ. In other words, for this to be valid it is necessary, but not even sufficient, that the composition of the wave packet remains unchanged over a distance at least equal to Λ.

Clearly this condition is not fulfilled when the subwave packet travels in a distorted region: over a distance Λ each of its components is shifted by an amount which can be estimated as $\tau(\Lambda)\sin\theta_B$; therefore, over a distance Λ, there is a change in the composition of the subwave packet, which means that Λ can no longer be viewed as the characteristic length, or spatial extension, of the considered phenomenon. We may alternatively say that, while travelling in the distorted crystal, the subwave packet 'picks up' new components, components which were not there in the perfect region.

Since what determines the shape of each subwave packet is the interference between all the plane-wave components which form it, we may conclude that *the shape of the subwave packet is altered* during its propagation in a distorted region. Moreover, since this change results from a broadening of the corresponding bump, we may even characterize this change as a *narrowing of the amplitude distribution* [see relation (1)].

The same holds *mutatis mutandis* along the x direction. We may therefore expect a narrowing of the 'beam' when it goes from a region of perfect crystal to a region of distorted crystal. This is clearly seen in Fig. 8 which shows the amplitude distribution at different depths of the 'beams' induced by a vacuum pseudo plane wave in a crystal containing a dislocation, as calculated on a computer from Takagi's equations (Epelboin, 1975). We see that each subwave packet shrinks while passing near the dislocation. The width of the amplitude distribution is narrower at the level indicated by the arrow than at the entrance surface. The wave packet then behaves like a wave which has been forced to pass through a very narrow slit, giving rise to an amplitude distribution which is characteristic of diffraction by a slit.

(c) Change in the modulation. Geometrical optics vs. wave optics

So far, we have been only concerned with the change supported by a single subwave packet. But it is

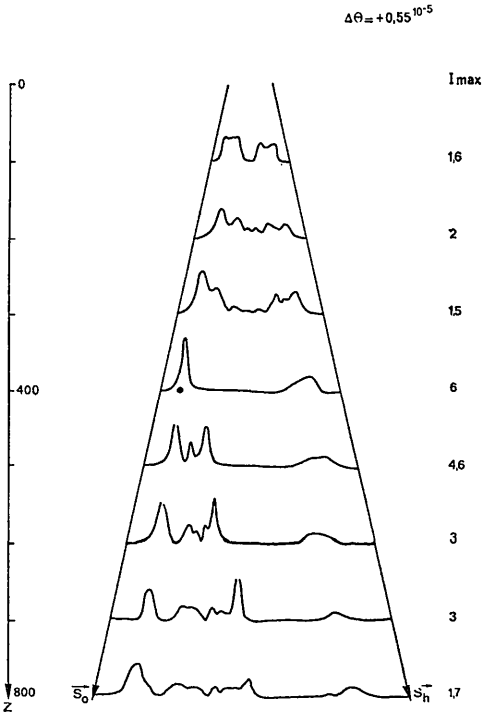

Fig. 8. Amplitude distribution (as calculated on a computer from Takagi's equations) at different depths in a crystal containing a single dislocation (the dark circle is the point where the dislocation line intersects the plane of incidence). A 'shrinking' of the amplitude distribution (or a 'narrowing' of the beam width) is clearly seen.

clear that a broadening in the two bumps along a given direction will also affect the distance between those bumps and therefore alter the modulation in the corresponding direction in reciprocal space.

As we have already said this effect will be more noticeable along K_z (and z) than along K_x (and x) because the ratio $\varrho = W/S$ is closer to 1 along the K_z direction than along the K_x direction.*

Let us consider as an example (which is also an extreme case) the case of an incident spherical wave. In the region of perfect crystal the K_z distribution is made up of two bumps of width $W \simeq 2\pi/\Lambda$ separated by a minimum distance $\simeq 2\pi/\Lambda$. We immediately see that the broadening of each bump following its entrance into the distorted region will be sufficient to make the two bumps join in a single bump. The question then arises whether we can still speak of a modulation (or Pendellösung in the X-ray case). This is a mere question of degree. We may state that if the broadening over a distance Λ is small as compared to the separation distance S the situation will not be very different from the perfect crystal case (as far as modulation or Pendellösung fringes are concerned).

In other words, as long as

$$\tau(\Lambda) \sin \theta_B \leq 2\pi/\Lambda \qquad (11)$$

the shape of each subwave packet is altered but the modulation (or Pendellösung) effect is not destroyed. This situation is exactly the same as the one pictured in Fig. 2(*b*). On the other hand, as soon as $\tau(\Lambda) \sin \theta_B$ becomes of the same order as the bump separation $2\pi/\Lambda$, the two bumps rejoin to form a single bump; the modulation effect disappears [see § II and Fig. 2(*c*)].

If we now want to visualize the situation with reference to the concept of ideal local dispersion surface, we see that starting from a K distribution localized on *one* branch of the dispersion surface we end with a distribution extending over *both* branches. In fact the concept of dispersion surface disappears; it does not make any sense to speak of a hyperbola when this hyperbola moves sufficiently fast so that over a distance equal to the spatial extension of the considered phenomenon, branch 1 comes where branch 2 used to be. We can also say that the dispersion surface is 'broadened' or 'thickened' in such a way that its two apices come close to one another. In other words the gap in the distribution disappears: the crystalline structure is so much altered that the gap (which we know from band theory is characteristic of a crystalline medium) disappears.

Returning to the crystal wave packet, we see that when the above condition is not fulfilled, the packet loses its characteristic structure and propagates in the form of two subwave packets; this structure is completely *destroyed.* This is a situation which is comparable to what happens in ordinary optics when diffraction of a plane wave (for instance) occurs: then the broadening of the K_z distribution is so large that the original shape of the wave is completely destroyed; from Huyghens theorem we know that we have to deal with a continuous sum of spherical waves over the aperture responsible for the diffraction, *i.e.* a continuous and large distribution of **K** vectors ('large' means large compared to the original distribution). By analogy we shall call *the above criterion* (11) the *criterion for validity of geometrical optics* in the case of X-ray propagation. Such a criterion has already been arrived at, in other ways, by one of us (Authier & Balibar, 1970). Let us now show for a special case and a constant gradient of deformation that the two criteria are identical.

The structure in two separate subwave packets characteristic of the perfect crystal is maintained as long as the broadening $\tau(\Lambda) \sin \theta_B$ undergone by each subwave packet is less than their separation $\simeq (2\pi/\Lambda).\tau(\Lambda)$ can be estimated as $|\nabla(\tau)|\Lambda$. Equations (9), (10) and the definition of f as the second derivative of $(\mathbf{g} \,.\, \mathbf{u})$ yield

$$\sin \theta_B \, \tau(\Lambda) \simeq \frac{1}{4 \cos \theta_B} f \Lambda \,. \qquad (12)$$

The maximum value of f is then estimated from (11) as

$$f \leq \frac{2\pi}{\Lambda^2} 4 \cos \theta_B \simeq K^2 \chi_h^2 \qquad (13)$$

$$\left(\text{since } \Lambda = \frac{\lambda \cos \theta_B}{C\sqrt{\chi_h \chi_{\bar{h}}}} \text{ in the symmetric case}\right).$$

The value of f in (13) is also the maximum value one obtains by applying the above-mentioned criterion for the validity of geometrical optics.

V. The so-called 'creation of new wave-fields'

This phenomenon is usually referred to as an explanation for the contrast of some fine details in dislocation images obtained by topography. Moreover, direct experimental evidence of this phenomenon has been given by Authier, Balibar & Epelboin (1970). Using a double spectrometer, the second crystal of which contains a single dislocation line, one can arrange that only one wave field propagates in the second crystal; it has been shown that this single wave field gives rise to two wave fields after it has travelled in the very distorted region surrounding the dislocation. We shall now examine this experiment in view of what we have said above.

A reasonable model for a crystal containing a single dislocation is the one of a very severely distorted zone sandwiched between two regions of perfect crystal. Normally, in the first good region, the energy propagates with the characteristic two-subwave-packet struc-

* The absolute value of the broadening is larger along K_x than along K_z by a factor $1/\text{tg}\,\theta_B \simeq 10$ but since the separation distance for the same incident $\delta K_0^{(1)}$ is $\Lambda/\lambda \simeq 10^6$ larger along K_x than along K_z, the ratio $\varrho = W/S$ will be more affected along K_z than along K_x.

ture; but, if we manage to eliminate one of these, we are left with a K_z distribution made up of a single narrow bump; this bump is narrow, because we assume a 'pseudo-plane' incident wave. While travelling in the distorted zone, this bump broadens as has been explained in § IV (*B*); the wave which leaves the distorted zone corresponds to a K_z distribution made up of a single large bump, which may, if the distortions are strong enough and extend over a large enough distance, extend in reciprocal space over a distance larger than Λ.

In the second good region where the concept of dispersion surface has some meaning the incident wave packet has an extension in reciprocal space larger than the separation between the two branches of the dispersion surface; therefore the extremities of some of its components lie outside the dispersion surface and thus cannot propagate. The good crystal then acts as a 'filter', and the K_z distribution is expected to '*shrink*' while going from the distorted region to the one of perfect crystal; this is just the reverse phenomenon of the one described in § IV and it results in a distribution with wave vectors lying on the dispersion surface. As distortions become less and less important, the large single bump gradually 'resolves' into two separate bumps, giving rise to the characteristic two subwave packets. In other words, starting with *one* 'wave field', we end with *two* 'wave fields'. But there is no reason why this second wave packet should have the same structure as the initial one; this latter was primarily determined by the shape of the incident vacuum wave packet, the essential features of which are lost in the broadening occuring in the distorted zone. On the other hand, the features of the subwave packet in the second good region are determined by these distortions rather than by anything else. Therefore we end with a completely different modulated Bloch-wave packet; or translated into the wave-field language: 'new wave fields are created'.

VI. Conclusion – a critique of the usual terminology

The considerations developed in §§ IV (*B*) and (*C*) make it clear that the widespread term 'wave field' is not adequate for a general description of X-ray propagation in distorted crystals. The wave-field concept is in fact closely related to the plane-wave approximation. Strictly speaking this word should be used only in the case of an incident plane wave and a perfect crystal. Using the proper concept (that of wave packet), we have shown that the term 'wave field' could be given an extended meaning as long as the wave packet maintains its structure in separated subwave packets (*i.e.* in the range of validity of 'geometrical optics'). Nevertheless it is impossible to give even an extended meaning to the word 'wave field' when this structure is lost. Then we have to deal with a K_z distribution with no particular structure and we must drop the usual terminology and the usual concept of dispersion surface related to it. This situation is bound to occur in strongly distorted crystals.

Moreover, we have shown that adoption of the wave-packet point of view provides a better insight into the phenomenon of 'creation of new wave fields'. As a matter of fact, the emergence, after propagation in strongly distorted regions, of 'wave fields' which did not belong to the composition of the initial wave packet must be viewed as one of the multiple avatars of this wave packet.

We end by proposing the following analogy: the *perfect* crystal acts as a wave splitter, in the same sense that one says that the Michelson apparatus is a beam splitter; the effect of crystal perfection is to split any incident wave packet into two separate K_z distributions which interfere. When the crystal becomes *imperfect*, it loses this characteristic property and even mixes components belonging to separate subwave packets, in the same way as in the Michelson-apparatus fringes fade out when the spectral distribution of the radiation becomes large compared to the path difference between the two beams.

References

AUTHIER, A. & BALIBAR, F. (1970). *Acta Cryst.* A**26**, 647–654.

AUTHIER, A., BALIBAR, F. & EPELBOIN, Y. (1970). *Phys. Stat. Sol.* **41**, 225–238.

BALIBAR, F. (1968). *Acta Cryst.* A**24**, 666–676.

BALIBAR, F. (1969). *Acta Cryst.* A**25**, 650–658.

BALIBAR, F. & AUTHIER, A. (1967). *Phys. Stat. Sol.* **21**, 413–421.

DARWIN, C. G. (1914). *Phil. Mag.* **27**, 315–333.

EPELBOIN, Y. (1975). Submitted to *Acta Cryst.*

EWALD, P. P. (1916). *Ann. Phys. Leipz.* **49**, 1–38.

KATO, N. (1963). *J. Phys. Soc. Japan*, **18**, 1785–1791.

KATO, N. (1964*a*). *J. Phys. Soc. Japan*, **19**, 67–77.

KATO, N. (1964*b*). *J. Phys. Soc. Japan*, **19**, 971–985; see also: AZAROFF, A., KAPLOW, R., KATO, N., WEISS, R. J., WILSON, A. J. C. & YOUNG, R. A. (1974). *X-Ray Diffraction.* New York: McGraw Hill.

LAUE, M. VON (1931). *Naturwissenschaften*, **10**, 133–158.

PENNING, P. (1966). Thesis, Delft.

PENNING, P. & POLDER, D. (1961). *Philips Res. Rep.* **16**, 419–440.

STERN, R. M., PENDRY, J. J. & BOUDREAUX, D. S. (1969). *Rev. Mod. Phys.* **41**, 275–295.

TAKAGI, S. (1962). *Acta Cryst.* **15**, 1311–1312.

TAKAGI, S. (1969). *J. Phys. Soc. Japan*, **27**, 1239–1253.

TAUPIN, D. (1964). *Bull. Soc. fr. Minér. Crist.* **87**, 469–511.